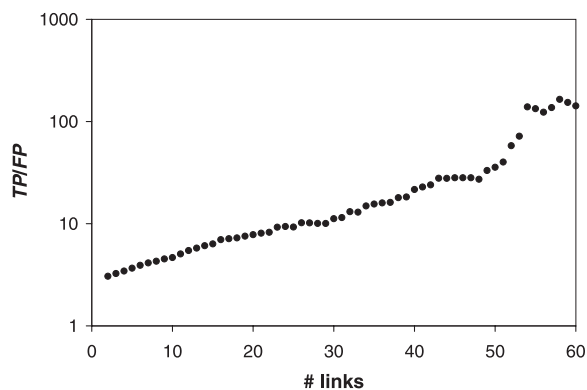


**Fig. 4.** *TP/FP* for subsets of the thresholded PIP that only include proteins with a minimum number of links. Requiring a minimum number of links isolates large complexes in the thresholded PIP graph (Fig. 3B). Increasing the minimum number of links raises *TP/FP* by preserving the interactions among proteins in large complexes, while filtering out false-positive interactions with heterogeneous groups of proteins outside the complexes.



The replication complex, a third experimental validation of the PIP, assembles and disassembles from transiently interacting subcomplexes (e.g., MCM proteins, ORC, and polymerases) throughout the cell cycle (8, 30). Our predicted and experimentally verified interactions connect it, probably transiently, to another subcomplex, replication factor A (RFA, composed of Rfa1, Rfa2, and Rfa3). Specifically, we predicted and verified interactions between RFA and two proteins associated with other replication subcomplexes: Rfa2 with Top2 (a component of the nuclear synaptonemal complex) and Rfa1 with Pri2 (DNA polymerase  $\alpha$ -primase subunit).

Finally, we predicted and verified by TAP-tagging that two proteins involved in translation elongation (Tef2 and Eft2) interact. This is plausible given that protein elongation is mediated by three factors in yeast: EF-1 $\alpha$  (Tef1, Tef2), EF-2 (Eft1, Eft2), and EF-3 (Hef3, Yef3); most other eukaryotes lack EF-3. Previous experimental data suggest an interaction between yeast EF-1 $\alpha$  and EF-3 (31). An interaction between EF-1 $\alpha$  and EF-2 had not been demonstrated, although this is reasonable given their similar roles in elongation and their overlapping binding sites on the ribosome (32).

In summary, we have developed a Bayesian approach for integrating weakly predictive genomic features into reliable predictions of protein-protein interactions. Our de novo prediction of complexes replicated interactions found in the gold-standard positives and PIE. In addition, we confirmed several of our predictions with new experiments. The accuracy of the PIP was comparable to that of the PIE while simultaneously achieving greater coverage.

Our procedure lends itself naturally to the addition of more features, possibly further improving results. We anticipate that protein-protein interactions in organisms other than yeast can be explored in similar ways.

#### References and Notes

1. P. Uetz et al., *Nature* **403**, 623 (2000).
2. T. Ito et al., *Proc. Natl. Acad. Sci. U.S.A.* **98**, 4569 (2001).
3. A. C. Gavin et al., *Nature* **415**, 141 (2002).
4. Y. Ho et al., *Nature* **415**, 180 (2002).
5. I. Xenarios et al., *Nucleic Acids Res.* **30**, 303 (2002).

6. H. W. Mewes et al., *Nucleic Acids Res.* **30**, 31 (2002).
7. G. D. Bader et al., *Nucleic Acids Res.* **29**, 242 (2001).
8. R. Jansen, D. Greenbaum, M. Gerstein, *Genome Res.* **12**, 37 (2002).
9. A. Kumar et al., *Genes Dev.* **16**, 707 (2002).
10. C. von Mering et al., *Nature* **417**, 399 (2002).
11. A. M. Deane, L. Salwinski, I. Xenarios, D. Eisenberg, *Mol. Cell. Proteomics* **1**, 349 (2002).
12. A. M. Edwards et al., *Trends Genet.* **18**, 529 (2002).
13. G. D. Bader, C. W. Hogue, *Nature Biotechnol.* **20**, 991 (2002).
14. A. Kumar, M. Snyder, *Nature* **415**, 123 (2002).
15. A. M. Marcotte, M. Pellegrini, M. J. Thompson, T. O. Yeates, D. Eisenberg, *Nature* **402**, 83 (1999).
16. M. Steffen, A. Petti, J. Aach, P. D'Haeseleer, G. Church, *BMC Bioinformatics* **3**, 34 (2002).

17. R. Jansen, N. Lan, J. Qian, M. Gerstein, *J. Struct. Funct. Genomics* **2**, 71 (2002).
18. A. Drawid, M. Gerstein, *J. Mol. Biol.* **301**, 1059 (2000).
19. Materials and methods are available as supporting material on Science Online.
20. T. R. Hughes et al., *Cell* **102**, 109 (2000).
21. R. J. Cho et al., *Mol. Cell* **2**, 65 (1998).
22. M. Ashburner et al., *Nature Genet.* **25**, 25 (2000).
23. See <http://genecensus.org/intint>.
24. I. P. Girard et al., *EMBO J.* **11**, 673 (1992).
25. N. K. Brewster, G. C. Johnston, R. A. Singer, *Mol. Cell. Biol.* **21**, 3491 (2001).
26. A. A. Travers, *EMBO Rep.* **4**, 131 (2003).
27. T. Formosa et al., *Genetics* **162**, 1557 (2002).
28. Y. Yu, P. Eriksson, L. T. Bhoite, D. J. Stillman, *Mol. Cell. Biol.* **23**, 1910 (2003).
29. R. C. Bash, J. M. Vargason, S. Cornejo, P. S. Ho, D. Lohr, *J. Biol. Chem.* **276**, 861 (2001).
30. O. M. Aparicio, D. M. Weinstein, S. P. Bell, *Cell* **91**, 59 (1997).
31. M. Anand, K. Chakraborty, M. J. Marton, A. G. Hinnebusch, T. G. Kinzy, *J. Biol. Chem.* **278**, 6985 (2003).
32. O. Kovalchuk, R. Kambampati, E. Pladies, K. Chakraborty, *Eur. J. Biochem.* **258**, 986 (1998).
33. We thank C. Sander and G. Bader for critical discussions.

#### Supporting Online Material

[www.sciencemag.org/cgi/content/full/302/5644/449/DC1](http://www.sciencemag.org/cgi/content/full/302/5644/449/DC1)

Materials and Methods

Figs. S1 to S3

Tables S1 and S2

References

29 May 2003; accepted 29 August 2003

## Transcriptional Repression of Atherogenic Inflammation: Modulation by PPAR $\delta$

Chih-Hao Lee,<sup>1</sup> Ajay Chawla,<sup>1\*</sup> Ned Urbiztondo,<sup>1</sup> Debbie Liao,<sup>1</sup> William A. Boisvert,<sup>2</sup> Ronald M. Evans<sup>1†</sup>

The formation of an atherosclerotic lesion is mediated by lipid-laden macrophages (foam cells), which also establish chronic inflammation associated with lesion progression. The peroxisome proliferator-activated receptor (PPAR)  $\gamma$  promotes lipid uptake and efflux in these atherogenic cells. In contrast, we found that the closely related receptor PPAR $\delta$  controls the inflammatory status of the macrophage. Deletion of PPAR $\delta$  from foam cells increased the availability of inflammatory suppressors, which in turn reduced atherosclerotic lesion area by more than 50%. We propose an unconventional ligand-dependent transcriptional pathway in which PPAR $\delta$  controls an inflammatory switch through its association and disassociation with transcriptional repressors. PPAR $\delta$  and its ligands may thus serve as therapeutic targets to attenuate inflammation and slow the progression of atherosclerosis.

Lipid-accumulating macrophages, or foam cells, are the major component of the atherogenic lesion. Loss of either of the

nuclear receptors PPAR $\gamma$  or liver X receptor (LXR)  $\alpha$  in the macrophage disables lipid export and accelerates progression of the atherosclerotic lesion (1–3), establishing a transcriptional basis for lipid homeostasis within coronary arteries (4, 5).

Synthetic ligands of the nuclear receptor PPAR $\delta$  (also called PPAR $\beta$ ) modulate lipid transport in monocytic cell lines through regulated expression of the scavenger receptor CD36 and the efflux pump ABCA1 (6, 7). By analogy with PPAR $\gamma$ , we hypothesized that loss of PPAR $\delta$  in macrophages may also disturb the dynamic balance of lipid uptake

<sup>1</sup>Howard Hughes Medical Institute, Gene Expression Laboratory, Salk Institute for Biological Studies, 10010 North Torrey Pines Road, La Jolla, CA 92037, USA. <sup>2</sup>Vascular Medicine Research, Brigham & Women's Hospital, 65 Landsdowne Street, Room 275, Cambridge, MA 02139, USA.

\*Present address: Division of Endocrinology, Metabolism and Gerontology, Department of Medicine, Stanford University, Stanford, CA 94305, USA.

†To whom correspondence should be addressed. E-mail: [evans@salk.edu](mailto:evans@salk.edu)

## REPORTS

and efflux, thereby aggravating disease progression. Because mice lacking the low-density lipoprotein receptor (LDLR<sup>-/-</sup> mice) readily develop atherosclerosis when fed a high-fat diet, the contribution of PPAR $\delta$  to cardiovascular disease can be evaluated in this mouse model by transplantation with PPAR $\delta$ <sup>-/-</sup> bone marrow.

We divided  $\gamma$ -irradiated LDLR<sup>-/-</sup> mice (C57/BL6 background) into three groups and then performed bone marrow transplants from wild-type C57/BL6, wild-type SV129, or PPAR $\delta$ <sup>-/-</sup> mice [high percentage chimera, SV129 background, >95% by fluorescence-activated cell sorting (8)]. The mice were then placed on an atherogenic diet for 8 weeks and quantitatively analyzed for lesion progression. Plasma total cholesterol levels were unchanged between the PPAR $\delta$ <sup>-/-</sup> bone marrow transplant (PPAR $\delta$ <sup>-/-</sup> BMT) mice and the two control BMT groups before or after the diet (fig. S1A). Similarly, lipid profiling revealed no difference in levels of very low density lipoprotein (VLDL), LDL, or high-density lipoprotein (HDL) between

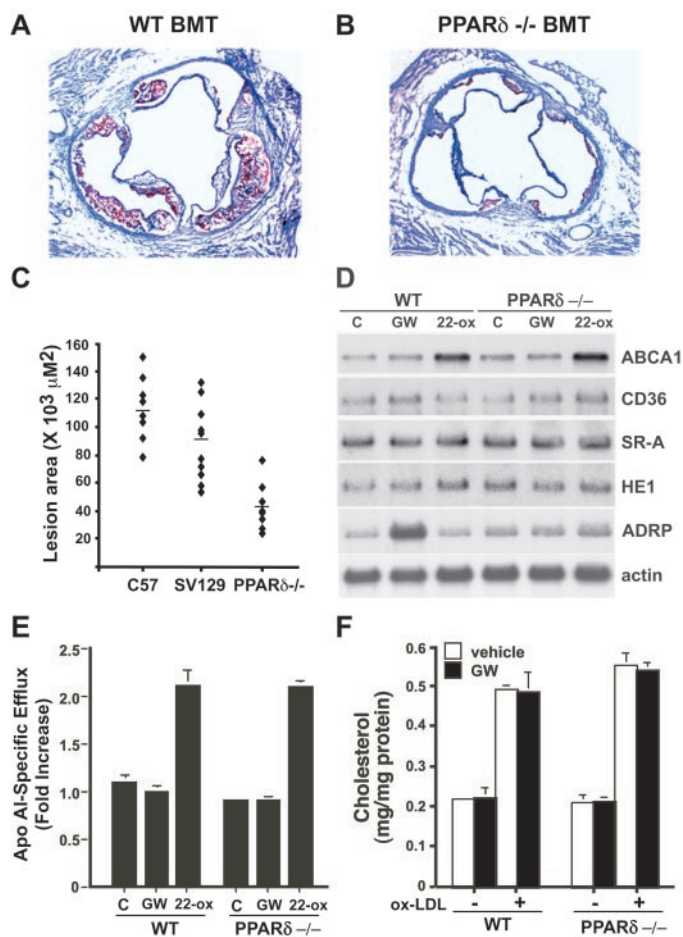
groups (8). However, analyses of the aortic valve sections revealed a drastic reduction in fatty streak in PPAR $\delta$ <sup>-/-</sup> BMT mice (Fig. 1, A and B). The average lesion area was 62% and 51% less in PPAR $\delta$  BMT mice than in the control BMT groups, respectively (Fig. 1C), making this one of the most striking protective effects among the nuclear receptor family described.

To determine whether the reduced lesion area in PPAR $\delta$ <sup>-/-</sup> BMT mice was due to an intrinsic inability of the macrophage to accumulate lipid, we examined macrophages derived from wild-type and PPAR $\delta$ <sup>-/-</sup> bone marrow. Wild-type and PPAR $\delta$ <sup>-/-</sup> cells expressed similar levels of scavenger receptors CD36 and SR-A and of endosomal cholesterol carrier HE1 (also called NPC2). Neither the expression of the ABCA1 transporter, which mediates reverse HDL transport, nor its activation by the LXR ligand 22-hydroxycholesterol (22-ox) was affected in the PPAR $\delta$ <sup>-/-</sup> cells (Fig. 1D). In contrast, ligand-induced activation of the direct target gene, ADRP (adipose

differentiation-related protein) (9), was abolished in the PPAR $\delta$ <sup>-/-</sup> macrophage. Interestingly, the basal level of ADRP was elevated in the null cells (Figs. 1D and 2A), suggesting a repression function for the unliganded receptor. In addition, cholesterol efflux mediated by Apo AI, the major cholesterol acceptor in HDL, was comparable between wild-type and PPAR $\delta$ <sup>-/-</sup> cells in the absence or presence of the PPAR $\delta$  synthetic agonist GW501516 (Fig. 1E). As a positive control, the LXR-specific ligands 22-ox or synthetic compound T0901317 (8) increased the efflux rate. Similarly, internalization of ox-LDL—which promotes macrophage inflammatory response, lipid accumulation, and lesion progression—induced cholesterol ester accumulation independent of PPAR $\delta$  or GW501516 (Fig. 1F) (fig. S1B). Collectively, these results suggest that PPAR $\delta$  does not appear to appreciably modulate either cholesterol uptake or efflux, and thus the observed lesion reduction in PPAR $\delta$ <sup>-/-</sup> BMT mice may not be a direct consequence of defects in cholesterol homeostasis.

In addition to accumulating lipid, macrophages are attracted to sites of tissue injury such as atherosclerotic lesions, where they elicit a chronic inflammatory response. To examine the inflammatory status of PPAR $\delta$ <sup>-/-</sup> macrophages, we examined the expression profile of proinflammatory genes in peritoneal macrophages (elicited by inflammatory agent thioglycollate). Northern blot analysis revealed that levels of monocyte chemoattractant protein MCP-1, cytokine IL-1 $\beta$  (interleukin-1 $\beta$ ), and matrix metalloproteinase MMP-9 were down-regulated in the PPAR $\delta$ <sup>-/-</sup> macrophage with or without ox-LDL stimulation (Fig. 2, A and B) (fig. S2A). Gene targeting studies of MCP-1 or its receptor CCR2 have shown that loss of either gene results in a 50 to 80% lesion reduction (10–13). In addition, both IL-1 $\beta$  and MMP-9 have been directly linked to lesion progression (14). However, the expression of other proinflammatory genes [such as those for tumor necrosis factor (TNF)  $\alpha$  and I $\kappa$ B kinase (IKK)  $\beta$ ] and of the transcriptional repressor BCL-6, which suppresses the production of multiple cytokines and chemokines including MCP-1, MCP-3, and macrophage inflammatory protein (MIP) 1 $\beta$  (15, 16), was similar between wild-type and PPAR $\delta$ <sup>-/-</sup> macrophages. A mouse macrophage cell line (RAW 264.7) stably overexpressing PPAR $\delta$  expressed higher levels of MCP-1, IL-1 $\beta$ , and MMP-9 relative to control cells (Fig. 2C). However, as seen in the peritoneal macrophage, TNF $\alpha$ , IKK $\beta$ , and BCL-6 expression remained unchanged. Overexpression of PPAR $\gamma$  in these cells had no effect on these target genes (8), consistent

**Fig. 1.** PPAR $\delta$ <sup>-/-</sup> bone marrow transplant suppresses atherosclerosis in the LDLR<sup>-/-</sup> mouse model. (A and B) Representative Oil Red O-stained sections of aortic valve from each group (magnification, 40 $\times$ ). Wild-type (WT) BMT mice (A) show more advanced, larger lesions than do PPAR $\delta$ <sup>-/-</sup> BMT mice (B). (C) The average lesion area was similar between C57/BL6 and SV129 control groups ( $P < 0.08$ , Mann-Whitney  $U$  test), whereas the PPAR $\delta$ <sup>-/-</sup> group lesion area was significantly reduced ( $P < 0.0003$ ). Lesion area means  $\pm$  SD: C57/BL6, 113,347  $\pm$  23,094  $\mu$ m<sup>2</sup> ( $n = 8$ ); SV129, 88,490  $\pm$  27,585  $\mu$ m<sup>2</sup> ( $n = 10$ ); PPAR $\delta$ <sup>-/-</sup>, 43,609  $\pm$  14,723  $\mu$ m<sup>2</sup> ( $n = 11$ ). (D) PPAR $\delta$  does not regulate genes involved in lipid uptake and efflux in the macrophage. Bone marrow-derived macrophages were treated with vehicle, PPAR $\delta$  synthetic ligand GW501516 (GW, 0.1  $\mu$ M), or LXR ligand 22-ox (5  $\mu$ M) for 24 hours. Total RNA was harvested and analyzed for gene expression on Northern blots. ABCA1, an LXR target gene, was induced by 22-ox in both WT and PPAR $\delta$ <sup>-/-</sup> cells. Actin probe is included as a loading control. (E) PPAR $\delta$ <sup>-/-</sup> cells exhibit a normal cholesterol efflux rate. SEMs from triplicate experiments are shown. (F) Lipids were extracted from macrophages with or without ox-LDL loading (25  $\mu$ g/ml, 24 hours). Cholesterol contents were determined with an enzymatic analysis kit.



with the competence of PPAR $\gamma$ <sup>-/-</sup> macrophages to respond to inflammatory stimuli (17). Immunohistochemical staining of the aortic valve section confirmed that PPAR $\delta$ <sup>-/-</sup> macrophages express a lower level of MCP-1 relative to wild-type macrophages (Fig. 2, D and E). These results suggest that MCP-1, IL-1 $\beta$ , and MMP-9 are critical PPAR $\delta$  targets that control macrophage inflammation and are associated with lesion reduction in the PPAR $\delta$ <sup>-/-</sup> BMT mice.

Although results from both PPAR $\delta$ <sup>-/-</sup> and PPAR $\delta$ -overexpressing macrophages suggest a proinflammatory role for PPAR $\delta$ , treatment of cells with GW501516 suppressed the expression of MCP-1 and IL-1 $\beta$  in a receptor-dependent manner, indicating that activation of PPAR $\delta$  is anti-inflammatory (Fig. 2, A and C). Moreover, MCP-1 expression in response to cytokine M-CSF (macrophage colony-stimulating factor) was compromised in PPAR $\delta$  null cells (as was also true for IL-1 $\beta$ , fig. S3A), and the addition of ligand in wild-type macrophages also reduced expression to levels similar to those of PPAR $\delta$ <sup>-/-</sup> cells (Fig. 3A). We also found that overexpression of PPAR $\delta$  (mediated by adenovirus) increased MCP-1 levels in the primary macrophage in a dose-dependent manner; this was completely reversed by ligand (Fig. 3B), which suggests that the amount of unliganded receptor determines MCP-1 expression.

We could not identify a functional PPAR $\delta$  response element within a 2.8-kb 5' regulatory region of the MCP-1 promoter, implying an indirect mechanism. As one plausible explanation, apo-PPAR $\delta$  could function as an MCP-1 activator by sequestering a negative regulator. Ligand activation could release the regulator, which would then repress MCP-1 expression. To test this hypothesis, we examined how expression of a mutant PPAR $\delta$  receptor (PPAR $\delta$  $\Delta$ AF2) that is deficient in the ligand-induced corepressor release affects MCP-1 expression. In principle, this mutant should bind the repressor but not release it in the presence of ligand. As expected, PPAR $\delta$  $\Delta$ AF2 is a potent inducer of MCP-1 but no longer shows ligand-induced suppression when expressed in RAW cells (Fig. 3C). As a control, GW501516 induced ADRP expression in cells expressing PPAR $\delta$  but not PPAR $\delta$  $\Delta$ AF2. A survey of chemokine expression revealed that MCP-3 and MIP-1 $\beta$  are also regulated by PPAR $\delta$  in a similar manner (Fig. 3, B and C). To determine whether this sequestering activity of PPAR $\delta$  is independent of DNA binding, we transfected RAW cells to express a fusion protein of the GAL4-PPAR $\delta$  ligand-binding domain (LBD) and a luciferase reporter containing the MCP-1 promoter. PPAR $\delta$ LBD and PPAR $\delta$  $\Delta$ AF2, but not

**Fig. 2.** PPAR $\delta$ <sup>-/-</sup> macrophages express lower levels of proinflammatory genes. (A and B) Northern blot analyses of peritoneal macrophages. Cells were treated with (+) or without (-) GW501516 (GW, 0.1  $\mu$ M) or ox-LDL (25  $\mu$ g/ml) for 24 hours. Actin served as a loading control. (C) Northern blot analysis of RNAs from control RAW cells [expressing yellow fluorescent protein (YFP)] or cells stably expressing PPAR $\delta$ . Overexpression of PPAR $\delta$  increases expression of proinflammatory genes, which could be reversed by ligand treatment. (D and E) Magnified (250 $\times$ ) images of aortic valve sections from WT and PPAR $\delta$ <sup>-/-</sup> BMT mice, respectively, stained with an antibody to mouse MCP-1 protein. The intensity of the red color corresponds to the expression level. Macrophages were identified by staining with MOMA-2, a cell surface marker (8).

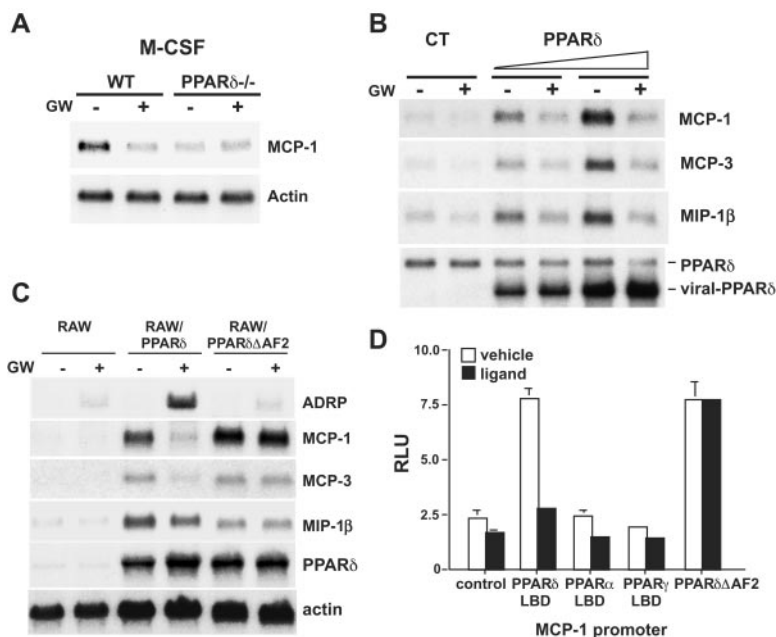
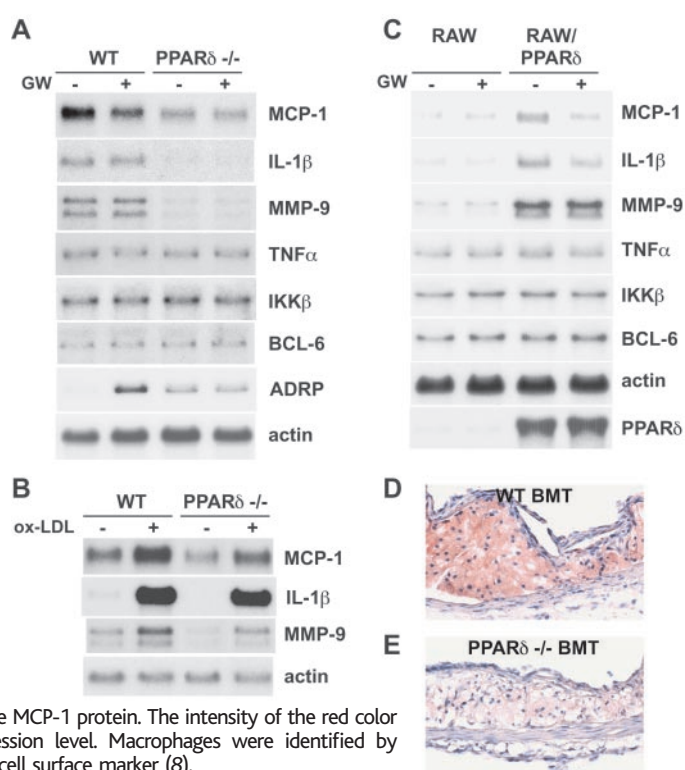


**Fig. 3.** PPAR $\delta$  exerts both pro- and anti-inflammatory activity. (A) A compromised response to M-CSF stimulation in PPAR $\delta$ <sup>-/-</sup> macrophages. Bone marrow-derived macrophages were withdrawn from differentiation medium for 1 day and restimulated with M-CSF (10 ng/ml) in the absence (-) or presence (+) of ligand GW501516 (GW) for 24 hours and analyzed for MCP-1 expression by Northern blots. (B) The pro- and anti-inflammatory activity of apo- and holo-PPAR $\delta$ . WT macrophages were transiently infected with adenovirus expressing YFP control (CT) or PPAR $\delta$ . GW501516 (GW) was added 2 days after infection and RNAs were collected for Northern analyses. Viral-PPAR $\delta$  transcript migrates at a lower position because it contains only the coding region. Endogenous PPAR $\delta$  transcript and actin (8) were used for the loading control. (C) Loss of ligand-mediated anti-inflammatory activity in the PPAR $\delta$  $\Delta$ AF2 mutant. RNAs from RAW cells stably expressing PPAR $\delta$  or PPAR $\delta$  $\Delta$ AF2 mutant in the absence (-) or presence (+) of ligand (GW) were analyzed for candidate gene expression by Northern blot. (D) Analyses of the PPAR $\delta$  sequestering effect on mouse MCP-1 promoter in RAW cells. RAW cells were transfected with a luciferase reporter containing a 2.8-kb MCP-1 promoter and expression vectors encoding either individual GAL4-PPAR LBD fusion protein or full-length PPAR $\delta$  $\Delta$ AF2 together with the heterodimer partner retinoid X receptor (RXR), along with a  $\beta$ -galactosidase internal control. The concentration for PPAR $\alpha$  ligand Wy14,643 was 30  $\mu$ M and PPAR $\gamma$  ligand rosiglitazone (BRL) was 1  $\mu$ M. Vehicle, dimethyl sulfoxide control; RLU, relative luciferase unit.

## REPORTS

PPAR $\alpha$ LBD or PPAR $\gamma$ LBD, increased reporter activity (Fig. 3D). Addition of ligand suppressed the effect of only PPAR $\delta$ LBD. Similar results were obtained with IL-1 $\beta$  promoter (fig. S3B). These data suggest that ligand activation can trigger an exchange between the corepressor and coactivator association with PPAR $\delta$ .

Because we observed an inverse correlation in regulating MCP-1, MCP-3, and MIP-1 $\beta$  expression between PPAR $\delta$  and the transcriptional repressor BCL-6 (16), we examined whether PPAR $\delta$  may act on BCL-6 either by direct binding or by corepressor competition. Immunoprecipitation of transfected 293 cells (human kidney epithelial cells) expressing epitope-tagged BCL-6 and PPAR $\delta$  indicated that the proteins interacted in a complex that was disrupted by PPAR $\delta$  ligand, whereas PPAR $\delta\Delta$ AF2 maintained interaction with

BCL-6 regardless of the ligand status (Fig. 4A). This suggests that BCL-6 and PPAR $\delta$  associate when PPAR $\delta$  is in its repressive mode. In contrast, PPAR $\alpha$  and PPAR $\gamma$  displayed almost no affinity for BCL-6. Deletion and truncation mutants of BCL-6 were generated to map the BCL-6–PPAR $\delta$  interaction domain in glutathione *S*-transferase (GST) pull-down assays. Immobilized GST or GST-PPAR $\delta$  fusion proteins were incubated with [<sup>35</sup>S]methionine-labeled BCL-6 truncation mutants and tested for their interactions. The BCL-6 zinc finger domain (amino acids 501 to 706) was both necessary and sufficient for binding to PPAR $\delta$  (Fig. 4B). Because class II histone deacetylase (HDAC) shares the same interaction domain in BCL-6 (18, 19), we examined whether PPAR $\delta$  association is competitive or compatible. GST-PPAR $\delta$  associated with BCL-6 alone as well as in the presence

of BCL-6–interacting proteins SMRT and HDAC7 (Fig. 4C), suggesting a potential extensive cross talk between these transcription factors. In addition, BCL-6 overexpression reversed the induction of MCP-1 promoter activity by apo-PPAR $\delta$  in transfected cells. However, it did not affect PPAR $\delta$  regulation of the ADRP promoter (Fig. 4, D and E). Thus, BCL-6 may be a key molecular target of PPAR $\delta$  in regulating macrophage chemokine and cytokine release.

Macrophages perform two important functions, lipid uptake and inflammation, in response to lipid insults at the vessel wall (20, 21). Insight into how members of the PPAR subfamily, which serve as lipid sensors, coordinate with each other to deal with such insults may assist the development of drugs for coronary artery diseases. We propose an unconventional ligand-dependent transcriptional pathway in which PPAR $\delta$  controls an inflammatory switch by virtue of its association (proinflammatory) and disassociation (anti-inflammatory) with transcriptional repressors (Fig. 4F). This pathway may become particularly important under inflammatory conditions when the corepressor pool is limited, as it has been shown that the inflammatory stimulus IL-1 $\beta$  causes nuclear export of a corepressor complex (22). However, given the complex nature of the atherosclerotic lesion (e.g., the composition of lipids and the involvement of various cytokines, chemokines, and cell types), further investigation is required to explore the contribution of PPAR $\delta$ /BCL-6 and other potential signaling pathways to the dynamic inflammatory status of the macrophage. Nonetheless, our findings suggest a consideration of PPAR $\delta$  modulators as a means to attenuate inflammation and slow the progression of atherosclerosis through a bona fide therapeutic pathway.

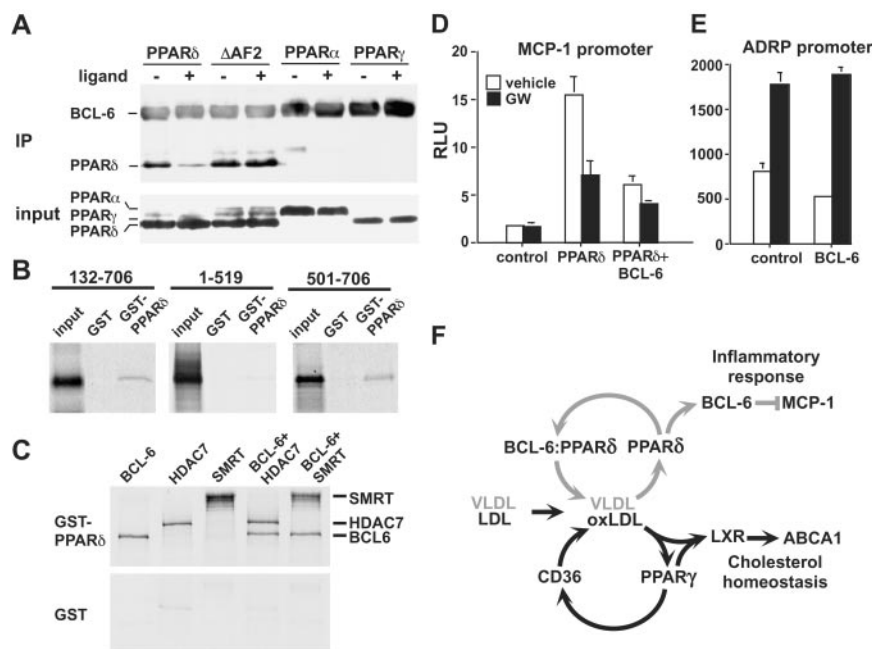


**Fig. 4.** (A) Unliganded PPAR $\delta$  interacts with BCL-6. Coimmunoprecipitation was performed in 293 cells transfected with PPARs (FLAG-tagged) and BCL-6 [hemagglutinin (HA)- and FLAG-tagged] in the absence (-) or presence (+) of ligand. Agarose beads conjugated with antibody to HA were used for immunoprecipitation. Protein interaction was analyzed by Western blots detected with an antibody to FLAG. IP, immunoprecipitation products; Input, 10% of cell lysate used for IP, showing expression levels of PPARs. (B and C) GST pull-down assays. BCL-6, BCL-6 truncation mutations, HDAC7, and SMRT (all in vitro translated and [<sup>35</sup>S]methionine labeled) were tested for interactions with GST-PPAR $\delta$  (bacterially expressed). Interaction complex was captured by glutathione-sepharose beads and resolved on an 8% SDS gel. GST alone was included as a negative control. Numbers in (B) correspond to amino acid residues of the human BCL-6 protein (19). Residues 501 to 706 contain the C-terminal zinc finger motif. Input: 10% of the [<sup>35</sup>S]methionine-labeled product. (D and E) Transient transfection experiments. RAW cells were transfected with a luciferase reporter containing either a MCP-1 or ADRP promoter (9) and expression vectors encoding PPAR $\delta$  and BCL-6. Overexpression of BCL-6 reversed the induction of MCP-1 promoter activity by the unliganded PPAR $\delta$  (D) but had no effect on the up-regulation of ADRP promoter by the liganded receptor (E). (F) Model for the differential regulatory network by PPAR $\delta$  and PPAR $\gamma$  in the macrophage. A PPAR $\gamma$ -LXR $\alpha$  regulatory cascade was previously shown to regulate lipid homeostasis (7). Here, an unconventional transcriptional pathway is proposed in which PPAR $\delta$  controls inflammation status by its association (proinflammatory) and disassociation (anti-inflammatory) with transcriptional repressors such as BCL-6. These observations suggest a division of labor within the macrophage, where PPAR $\gamma$  and PPAR $\delta$  provide distinct points of transcriptional control of genes regulating cholesterol homeostasis and inflammation, respectively.

## References and Notes

1. A. Chawla *et al.*, *Mol. Cell* **7**, 161 (2001).
2. S. B. Joseph *et al.*, *Proc. Natl. Acad. Sci. U.S.A.* **99**, 7604 (2002).
3. R. K. Tangirala *et al.*, *Proc. Natl. Acad. Sci. U.S.A.* **99**, 11896 (2002).
4. C. H. Lee, R. M. Evans, *Trends Endocrinol. Metab.* **13**, 331 (2002).
5. J. J. Repa, D. J. Mangelsdorf, *Nature Med.* **8**, 1243 (2002).
6. H. Vosper *et al.*, *J. Biol. Chem.* **276**, 44258 (2001).
7. W. R. Oliver Jr. *et al.*, *Proc. Natl. Acad. Sci. U.S.A.* **98**, 5306 (2001).
8. C. H. Lee, R. M. Evans, unpublished data.
9. A. Chawla *et al.*, *Proc. Natl. Acad. Sci. U.S.A.* **100**, 1268 (2003).
10. J. Gosling *et al.*, *J. Clin. Invest.* **103**, 773 (1999).
11. L. Gu *et al.*, *Mol. Cell* **2**, 275 (1998).
12. T. C. Dawson, W. A. Kuziel, T. A. Osahar, N. Maeda, *Atherosclerosis* **143**, 205 (1999).
13. L. Boring, J. Gosling, M. Cleary, I. F. Charo, *Nature* **394**, 894 (1998).
14. A. C. Li, C. K. Glass, *Nature Med.* **8**, 1235 (2002).
15. A. L. Dent, A. L. Shaffer, X. Yu, D. Allman, L. M. Staudt, *Science* **276**, 589 (1997).
16. L. M. Toney *et al.*, *Nature Immunol.* **1**, 214 (2000).
17. A. Chawla *et al.*, *Nature Med.* **7**, 48 (2001).

18. K. D. Huynh, W. Fischle, E. Verdin, V. J. Bardwell, *Genes Dev.* **14**, 1810 (2000).  
 19. C. Lemerrier *et al.*, *J. Biol. Chem.* **277**, 22045 (2002).  
 20. C. J. Binder *et al.*, *Nature Med.* **8**, 1218 (2002).  
 21. D. Steinberg, *Nature Med.* **8**, 1211 (2002).  
 22. S. H. Baik *et al.*, *Cell* **110**, 55 (2002).  
 23. We thank J. L. Witztum, C. K. Glass, P. Tontozov, W. Alaynick, P. Olson, and R. Nofsinger for valuable comments; R. Yu, M. Downes, Y. Wang, and W. He for

reagents; I. Mehl for Q-PCR analyses; L. K. Curtiss and A. S. Black for assistance in macrophage differentiation; A. L. Dent for pGCN-BCL-6 plasmid; H.-Y. Kao for BCL-6 deletion plasmids; and E. Stevens and L. Ong for administrative assistance. R.M.E. is an investigator of the Howard Hughes Medical Institute at the Salk Institute for Biological Studies and March of Dimes Chair in Molecular and Developmental Biology. Supported by the Howard Hughes Medical Institute (R.M.E.) and NIH grant HL69474 (W.A.B.).

#### Supporting Online Material

www.sciencemag.org/cgi/content/full/1087344/DC1  
 Materials and Methods  
 Figs. S1 to S3  
 References and Notes

5 May 2003; accepted 26 August 2003  
 Published online 11 September 2003;  
 10.1126/science.1087344

Include this information when citing this paper.

## Hybridization Between *Brassica napus* and *B. rapa* on a National Scale in the United Kingdom

Mike J. Wilkinson,<sup>1\*</sup> Luisa J. Elliott,<sup>2</sup> Joël Allainguillaume,<sup>1</sup>  
 Michael W. Shaw,<sup>1</sup> Carol Norris,<sup>3</sup> Ruth Welters,<sup>4</sup> Matthew  
 Alexander,<sup>4</sup> Jeremy Sweet,<sup>3</sup> David C. Mason<sup>2</sup>

Measures blocking hybridization would prevent or reduce biotic or environmental change caused by gene flow from genetically modified (GM) crops to wild relatives. The efficacy of any such measure depends on hybrid numbers within the legislative region over the life-span of the GM cultivar. We present a national assessment of hybridization between rapeseed (*Brassica napus*) and *B. rapa* from a combination of sources, including population surveys, remote sensing, pollen dispersal profiles, herbarium data, local Floras, and other floristic databases. Across the United Kingdom, we estimate that 32,000 hybrids form annually in waterside *B. rapa* populations, whereas the less abundant weedy populations contain 17,000 hybrids. These findings set targets for strategies to eliminate hybridization and represent the first step toward quantitative risk assessment on a national scale.

Globally, cultivation of genetically modified (GM) crops has increased to 59 Mha in 2002 (1). GM cultivars offer economic and environmental benefits (2), but also raise concerns that hybridization with wild relatives could cause unwanted environmental change (3, 4). Several strategies could suppress hybridization between GM crops and wild relatives, including physical isolation (5), male sterility (6), “safe” integration sites (7), molecular control systems (8), and chloroplast transformation (9). These approaches have variable capacity to inhibit hybridization, and their utility depends on hybrid numbers expected in the target legislative region. Probability of change in a specified time interval increases with the number of hybrids formed, because some hybrids with the potential to cause change will not survive (10). It is therefore desirable to quantify hybrid formation on the legislative scale.

After commercialization in the United Kingdom (UK), GM rapeseed is most likely to hybridize with *B. rapa* (11). *B. rapa* occurs commonly in wild populations near waterways

and infrequently as an agricultural weed. These “ecotypes” are considered separately. Hybrids between these species occur spontaneously (12), although there is currently no basis on which to estimate numbers nationally. To achieve such an estimate, we consider hybrids formed at sympatric sites and hybrids arising from long-range pollination.

Waterside *B. rapa* populations occupy seminatural communities with broad scope for ecological change after transgene recruitment. We inferred sympatry between these species by combining the mean density of *B. rapa* plants on waterways containing the species with the number of waterside rapeseed fields.

Rapeseed (Fig. 1A) and wild *B. rapa* (13) are almost absent from Northern Ireland, so our work focused on mainland Britain. We identified *B. rapa* on 95 British river systems by reference to local Floras, the database of the Botanical Society of the British Isles, the Centre for Ecology and Hydrology (CEH) Countryside Survey 2000, 591 herbarium specimens, and by direct surveying (13) (fig. S1). All sources indicated the absence of riverbank *B. rapa* from Scotland (13). For instance, none of the 57 Scottish herbarium specimens were from rivers, and 16 Scottish local Floras made no mention of riverside *B. rapa* (13). Size and position of waterside *B. rapa* populations elsewhere was surveyed along 151 km of nine riverbanks and 165 km of four canals (13). *B. rapa* was mark-

edly more common on riverbanks (0.755 plants/m) than on canals (0.0037 plants/m). Sympatry was calculated separately for each. First, 95% confidence intervals for plant density were calculated as 0.31 to 1.81 plants/m for rivers and 0.0014 to 0.0096 plants/m for canals (13). An altitudinal limit of 155 m was set for riverside *B. rapa* after surveying eight rivers to their sources (13). *B. rapa* was also absent from brackish water (13). These parameters were applied to all waterways containing *B. rapa* to predict distribution of waterside populations (Fig. 1B).

River confluences with *B. rapa* totaled 117 Mm (13), on which we expect 88 million riverbank *B. rapa* plants (117 Mm × 0.755 plants/m), with a broad 95% confidence range of 37 million to 211 million plants. Canals contribute a comparatively negligible 79,000 plants (95% confidence range: 30,000 to 204,000 plants). We determined the length of rivers and canals within 30 m (one satellite image pixel) of rapeseed, primarily by overlaying satellite images covering areas of highest rapeseed and riverside *B. rapa* incidence with digitized waterways data (13). The number of sympatric plants was calculated as the product of riverbank length within 30 m of rapeseed and mean density of waterway *B. rapa*. Sympatry in residual areas outside satellite imagery (25% of total) was calculated by regression (13). Combination of both elements provided a spatially explicit profile of sympatry (Fig. 1C). We thus estimate that 1.8 million waterside *B. rapa* plants are within 30 m of rapeseed fields in the UK. We empirically calculated hybridization rates at sites of sympatry. We identified 47 hybrids among 3230 plants from eight sympatric populations (13, 14). Given 1.8 million sympatric *B. rapa* plants and this hybridization rate of 1.46% (±0.43%, 2 SEM Poisson error estimate), we estimate 26,000 (±22,000, 2 SEM) hybrids within sympatric waterside *B. rapa* populations.

We based long-range hybridization estimates on airborne pollen dispersal profiles. This assumes that long-range pollination by bees is negligible or similar to wind pollination but only underestimates gene flow should bee-mediated long-range dispersal exceed that by wind. Reexamination of airborne pollen profiles from isolated rapeseed fields over 2 years (15) revealed pollen density ( $p$ ), which can be described as

$$p(x) = \frac{e^{-x/l}}{C(c + x)^b}$$

<sup>1</sup>School of Plant Sciences, The University of Reading, RG6 6AS, UK. <sup>2</sup>Natural Environment Research Council Environmental Systems Science Centre, The University of Reading, RG6 6AL, UK. <sup>3</sup>NIAB, Cambridge CB3 0LE, UK. <sup>4</sup>Centre for Ecology and Hydrology, Winton, Dorset, UK.

\*To whom correspondence should be addressed. E-mail: m.j.wilkinson@rdg.ac.uk